

Massachusetts Institute of Technology
Space Systems Laboratory

April 15, 1999

Research Contract No. NAG5-7839
Memorandum MIT-SSL-NGST-99-1

Title: **Low Order Space Observatory Sample Problem (Part I)**
A simple three-degree of freedom analytical “testbed” for the exploration of basic concepts in integrated modeling, disturbance analysis and parameter sensitivity analysis.

Part I: Integrated Modeling

Summary:

A simple three degree of freedom sample problem of a precision opto-mechanical system was developed and solved. This is the first part of a series of memos that explore the insights to be gained from this kind of simplified analytical problem. Integrated modeling, as presented in this first part, is understood to be the assembly and analysis of an overall system model, containing structures, optics and controls subsystems.

Four goals are pursued with this sample problem. Firstly the problem is of didactic value since it derives the fundamental equations for integrated dynamics modeling and thus serves as a useful introduction to the field. Secondly the problem was used to explore the different methods for predicting RMS (root-mean-square) performance values for an opto-mechanical system. Thirdly the solutions were used to analytically validate the accuracy of disturbance analysis and sensitivity analysis software tools previously developed by Gutierrez, Kenny et alteri. And lastly the sample problem serves to pave the way for further developments such as the future implementation of sensitivity analyses with respect to disturbance filter or control parameters or the simultaneous optimization of the structures/controls/optics design

Distribution: Gary E. Mosier, NASA Goddard Space Flight Center
Bob Grogan, NASA Jet Propulsion Laboratory
Prof. David Miller, R. Masterson, S. Uebelhart, G. Mallory

Author: Olivier de Weck
Space Systems Laboratory, Room 37-391
Massachusetts Institute of Technology
77 Massachusetts Avenue, Cambridge, MA 02458
Phone: (617) 253-3267, Fax: (617) 258-5940
Email: deweck@mit.edu, URL: <http://web.mit.edu/ssl/ngst>

Abstract

A linear three-degree of freedom problem representing a precision opto-mechanical system in space was developed. The goal of this problem is to convey the fundamentals of integrated modeling for dynamics and control in a concise and rigorous manner and to illustrate the methodology of conceptual design analysis. Furthermore the results are used to verify the correctness of a performance assessment and enhancement framework, that was developed at the Space Systems Laboratory [1]. First a conceptual model of a linear space interferometer with 2 collectors and 1 central combiner is developed. The combiner and collectors are modeled as concentrated masses connected by axial springs. Secondly the structural model is obtained by solving the generalized eigenvalue problem and assembling the corresponding state space system in 2nd order modal form. A dynamic disturbance acts at the central mass and can be characterized as a random white noise source filtered by a low-bass or alternatively by a band-pass shaping filter. The optics model consists of a linear sensitivity matrix that relates the physical displacements of the structure to the optical pathlength difference (OPD). Finally a low-impedance force actuator on one of the two springs is modeled in order to improve the performance with the help of a laser metrology sensor and a PD-controller. The integrated modeling process then consists in assembling all the sub-models into an overall state space system and analyzing its stability.

The key feature of this sample problem is that it is tractable analytically (i.e. pencil and paper calculations) as well as numerically with existing MATLAB™ based analysis tools. The principles and equations presented here are applicable to a wide range of modeling problems such as the Next Generation Space Telescope (NGST), the Space Interferometry Mission (SIM) or the Terrestrial Planet Finder (TPF) mission.

Convention: Matrices and vectors are printed in **bold** letters and symbols

1. Conceptual System Model

The conceptual model that has been developed for this study is shown schematically in figure 1. The layout is representative of a space interferometer with two identical collectors, that are structurally connected with the central mass containing the combiner optics and the spacecraft bus. Alternatively the system could represent an observatory with a large aperture primary mirror and a central bus containing the science instruments and utility functions. The path of stellar light from the apertures to the combiner is shown in gray.

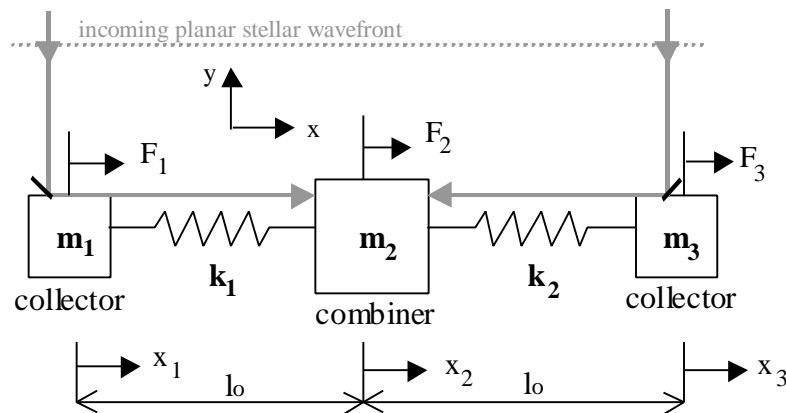


Fig. 1: Conceptual model of opto-mechanical system with three degrees of freedom

A number of assumptions underlie the model presented in figure 1. We are only interested in translational motion in the x -direction of the spacecraft coordinate frame. As a matter of simplification we set $m_1 = m_3 = m$. It is reasonable to assume that the combiner is more massive than the collectors and we set $m_2 = 4m$. The mass of the compliant structure is neglected, the axial stiffness however is represented by identical linear springs $k_1 = k_2 = k$, that will be assigned realistic properties based on equivalent truss properties. The reference length of each arm is l_0 , which will only enter into the expression for the equivalent stiffness k .

2. Structural modeling

The first step in dynamics modeling, regardless of the precise nature of the problem is to formulate the equations of motion of the system in an appropriate reference frame. For complex

motions and geometries the energy methods, such as the Lagrange approach are very powerful. In the present case the equations of motion can be formulated directly by looking at the freebody diagram for each mass.

$$\begin{aligned}
 m_1 \ddot{x}_1 &= (x_2 - x_1)k_1 + F_1 \\
 m_2 \ddot{x}_2 &= -(x_2 - x_1)k_1 + (x_3 - x_2)k_2 + F_2 \\
 m_3 \ddot{x}_3 &= -(x_3 - x_2)k_2 + F_3
 \end{aligned}
 \tag{1}$$

It shall be noted that these equations represent a linear system of 2nd order, coupled differential equations. The coupling makes these equations challenging to solve in the present form. These equations are then conveniently rewritten in matrix form as,

$$\underbrace{\begin{bmatrix} m_1 & 0 & 0 \\ 0 & m_2 & 0 \\ 0 & 0 & m_3 \end{bmatrix}}_{\mathbf{M}} \underbrace{\begin{bmatrix} \ddot{x}_1 \\ \ddot{x}_2 \\ \ddot{x}_3 \end{bmatrix}}_{\ddot{\mathbf{x}}} + \underbrace{\begin{bmatrix} k_1 & -k_1 & 0 \\ -k_1 & k_1 + k_2 & -k_2 \\ 0 & -k_2 & k_2 \end{bmatrix}}_{\mathbf{K}} \underbrace{\begin{bmatrix} x_1 \\ x_2 \\ x_3 \end{bmatrix}}_{\mathbf{x}} = \underbrace{\begin{bmatrix} F_1 \\ F_2 \\ F_3 \end{bmatrix}}_{\mathbf{F}}
 \tag{2}$$

$$\mathbf{M} \ddot{\mathbf{x}} + \mathbf{K} \mathbf{x} = \mathbf{F}
 \tag{3}$$

where **M** and **K** are the global mass and stiffness matrix respectively and **F** is the vector of external forces. It shall be noted that (3) does not contain an explicit damping matrix **C**, as might be expected since all structures and materials experience some amount of damping, that is due to the irreversible dissipation of mechanical energy from the system due to structural motion. Damping is typically added at a later stage of the modeling process [2]. The forces **F** arise from a superposition of disturbance and control actuator forces. We are assuming that the spring constants of both springs are equal and can be computed from the axial stiffness of an equivalent truss structure.

$$k_1 = k_2 = k = \frac{EA}{l_o}
 \tag{4}$$

A set of initial model properties was chosen for this sample problem in table 1. The values are based on realistic structures. It will be the goal of future research to apply optimization algorithms to these nominal values in order to optimize performance within given bounds of the material properties.

Mass parameter m	200 kg
Young's modulus E^1	$7.1 \cdot 10^{10}$ N/m ²
Cross sectional area A^2	0.001 m ²
Reference length l_0	10 m

Table 1: Sample problem nominal model properties

The various simplifications from above can be applied and we obtain:

$$\underbrace{\begin{pmatrix} m & 0 & 0 \\ 0 & 4m & 0 \\ 0 & 0 & m \end{pmatrix}}_{\mathbf{M}} \underbrace{\begin{pmatrix} \ddot{x}_1 \\ \ddot{x}_2 \\ \ddot{x}_3 \end{pmatrix}}_{\ddot{\mathbf{x}}} + \underbrace{\begin{pmatrix} k & -k & 0 \\ -k & 2k & -k \\ 0 & -k & k \end{pmatrix}}_{\mathbf{K}} \underbrace{\begin{pmatrix} x_1 \\ x_2 \\ x_3 \end{pmatrix}}_{\mathbf{x}} = \underbrace{\begin{pmatrix} F_1 \\ F_2 \\ F_3 \end{pmatrix}}_{\mathbf{F}} \tag{2a}$$

M: global mass matrix

F: vector of applied forces

K: global stiffness matrix

x: vector of physical displacements

For a linear elastic static analysis we assume that the accelerations of the structure $\ddot{\mathbf{x}}$, that give rise to the inertial forces are negligible. The remaining system of linear equations $\mathbf{K}\mathbf{x} = \mathbf{F}$ can be solved easily provided the problem is well posed. Methods that use triangularization such as Gauss-Jordan elimination are preferable to inversion of the stiffness matrix. It is true however that the \mathbf{K} matrix needs to be non-singular for the problem to have a unique solution. A normal modes analysis is then performed if we do not neglect the accelerations $\ddot{\mathbf{x}}$. This is done to gain insight into the dynamic behavior of the structure. We assume a periodic unforced response at each degree of freedom of the form [5]:

¹ Elastic modulus of aluminum [3]

² Corresponds to 10 cm² cross sectional area, reasonable value for a large space truss [4]

$$x_i = e^{j\omega t} \quad , \quad i = 1, 2, 3 \tag{5}$$

Substituting (5) in (2a) we can write the following expression,

$$\begin{pmatrix} mj^2\omega^2 & 0 & 0 \\ 0 & 4mj^2\omega^2 & 0 \\ 0 & 0 & mj^2\omega^2 \end{pmatrix} e^{j\omega t} + \begin{pmatrix} k & -k & 0 \\ -k & 2k & -k \\ 0 & -k & k \end{pmatrix} e^{j\omega t} = \begin{pmatrix} 0 \\ 0 \\ 0 \end{pmatrix} \tag{6}$$

since we assume that $e^{j\omega t} \neq 0$ and by substituting $\mathbf{I} = \omega^2$ and $j^2 = -1$ we obtain the formulation for the generalized eigenvalue problem,

$$[\mathbf{K} - \mathbf{I}_i \mathbf{M}] \cdot \mathbf{f}_i = 0 \tag{7}$$

where λ_i is the i-th eigenvalue of the structure (square of the natural vibration frequency in rad/sec) and ϕ_i is the i-th eigenvector. The ϕ_i 's are the columns of the matrix Φ , which is sometimes referred to as the modeshape matrix. First the eigenvalues are computed by setting the determinant of $[\mathbf{K} - \lambda_i \mathbf{M}]$ to zero.

$$\det[\mathbf{K} - \mathbf{I} \mathbf{M}] = \det \begin{pmatrix} k - \mathbf{I}m & -k & 0 \\ -k & 2k - 4\mathbf{I}m & -k \\ 0 & -k & k - \mathbf{I}m \end{pmatrix} = 0 \tag{8}$$

After evaluating the determinant and some algebra we obtain a polynomial of degree $n = 3$, which can be solved for the eigenvalues λ .

$$-2m^2 \mathbf{I}^3 + 5km \mathbf{I}^2 - 3k^2 \mathbf{I} = 0 \tag{9a}$$

We can factor out λ and multiply by (-1) so that the following expression is obtained:

$$\mathbf{I} (2m^2 \mathbf{I}^2 - 5km \mathbf{I} + 3k^2) = 0 \tag{9b}$$

It becomes immediately clear that one of the eigenvalues is $\lambda_1 = 0$. This eigenvalue corresponds to the translational rigid body mode in the x-direction as will be seen later. The remaining quadratic equation in brackets can be solved easily to yield,

$$I_{2,3} = \frac{5km \pm \sqrt{25k^2m^2 - 24k^2m^2}}{4m^2} = \frac{5km \pm km}{4m^2} = \frac{5k \pm k}{4m} \quad (10)$$

so that we have three distinct and real eigenvalues, that we can evaluate by substituting the previously determined physical model properties (table 1) for the stiffness k and the mass m.

$$\begin{aligned} I_1 &= 0 = 0 \left[\frac{\text{rad}^2}{\text{sec}^2} \right] \\ I_2 &= \frac{4km}{4m^2} = \frac{k}{m} = 35500 \left[\frac{\text{rad}^2}{\text{sec}^2} \right] \\ I_3 &= \frac{6km}{4m^2} = \frac{3k}{2m} = 53250 \left[\frac{\text{rad}^2}{\text{sec}^2} \right] \end{aligned} \quad (11)$$

The natural frequencies in cycles per second [Hz] are the square root of the eigenvalues divided by 2π :

$$\begin{aligned} f_1 &= \frac{w_1}{2p} = \frac{\sqrt{I_1}}{2p} = 0 \quad [\text{Hz}] \\ f_2 &= \frac{w_2}{2p} = \frac{\sqrt{I_2}}{2p} = 29.99 \quad [\text{Hz}] \\ f_3 &= \frac{w_3}{2p} = \frac{\sqrt{I_3}}{2p} = 36.73 \quad [\text{Hz}] \end{aligned} \quad (12)$$

It was mentioned that the first mode at 0 Hz is the rigid body mode, but the question remains what behavior the other two modes exhibit. This question can be answered by computing the corresponding eigenvectors f_i .

$$[\mathbf{K} - I_1 \mathbf{M}] \cdot \mathbf{f}_1 = 0 = \begin{bmatrix} k & -k & 0 \\ -k & 2k & -k \\ 0 & -k & k \end{bmatrix} \begin{bmatrix} f_{11} \\ f_{21} \\ f_{31} \end{bmatrix} = 0, \quad \text{thus } \mathbf{f}_1 = \begin{bmatrix} 1 \\ 0 \\ 0 \end{bmatrix} \quad (13a)$$

$$[\mathbf{K} - I_2 \mathbf{M}] \cdot \mathbf{f}_2 = 0 = \begin{bmatrix} 0 & -k & 0 \\ -k & 2k & -k \\ 0 & -k & 0 \end{bmatrix} \begin{bmatrix} f_{12} \\ f_{22} \\ f_{32} \end{bmatrix} = 0, \quad \text{thus } \mathbf{f}_2 = \begin{bmatrix} 1 \\ 0 \\ -1 \end{bmatrix} \quad (13b)$$

$$[\mathbf{K} - I_3 \mathbf{M}] \cdot \mathbf{f}_3 = 0 = \begin{bmatrix} k/2 & -k & 0 \\ -k & -4k & -k \\ 0 & -k & -k/2 \end{bmatrix} \begin{bmatrix} f_{13} \\ f_{23} \\ f_{33} \end{bmatrix} = 0, \quad \text{thus } \mathbf{f}_3 = \begin{bmatrix} 2 \\ -1 \\ 2 \end{bmatrix} \quad (13c)$$

When solving for the eigenvectors it becomes clear that $[\mathbf{K} - \lambda_i \mathbf{M}]$ is not positive definite, since the λ_i 's are by definition all solutions to the characteristic equation. Thus the magnitude of the eigenvectors is not uniquely defined. If however we choose one of the entries of the eigenvector arbitrarily, then all other entries are automatically defined. We will turn to the matter of normalization of the eigenvectors later in this section. The eigenvectors are the columns of the modeshape matrix \mathbf{F} .

$$\mathbf{F} = [\mathbf{f}_1 | \mathbf{f}_2 | \mathbf{f}_3] = \begin{bmatrix} 1 & 1 & 2 \\ 0 & 0 & -1 \\ -1 & -1 & 2 \end{bmatrix}, \quad \text{and} \quad \mathbf{F}^T = \begin{bmatrix} f_1^T \\ f_2^T \\ f_3^T \end{bmatrix} = \begin{bmatrix} 1 & 1 & 1 \\ 1 & 0 & -1 \\ 2 & -1 & 2 \end{bmatrix}. \quad (14)$$

The physical interpretation of the eigenvectors as modeshapes is based on the underlying notion that the relative magnitudes of the components of the eigenvector correspond to the modeshape, i.e. the dynamic displacements occurring at that particular natural frequency. In the present case we can schematically depict the system behavior for the three modes of interest (figure 2).

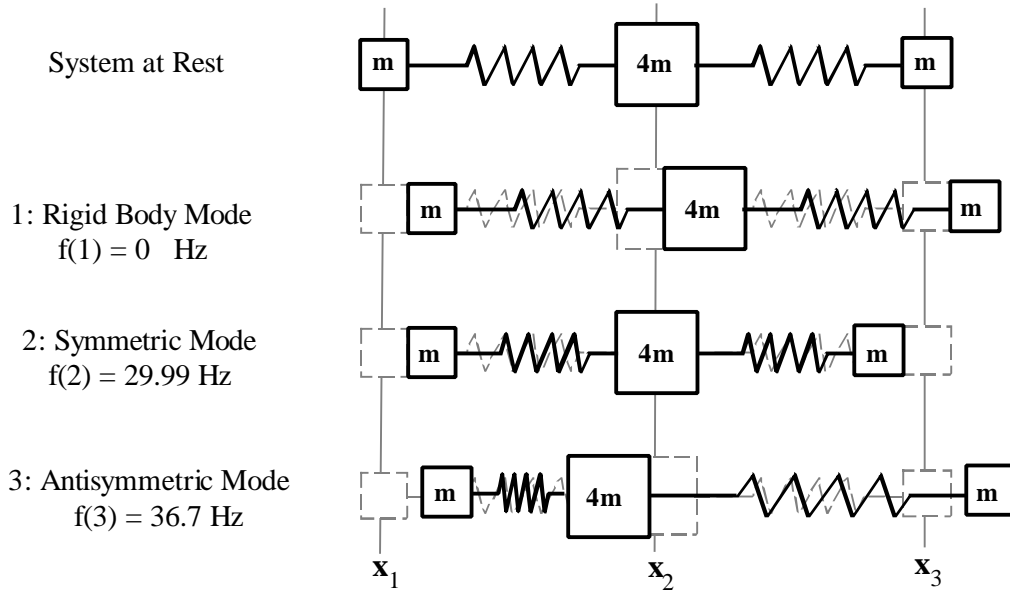


Fig. 2: Mode shape visualization for sample problem

It can be seen that the displacements are all equal in the rigid body mode so that every component of the structure experiences uniform translation. Since there are no relative displacements, the system contains no strain energy. For mode number 2 (the first flexible mode) we have symmetric deflections of the two aperture nodes, so that both springs are in tension or in compression at the same time. The third mode is characterized by anti-symmetric deflections of the aperture nodes, so that while one spring is in compression, the other spring will be in tension and vice versa.

It is useful and customary to normalize the columns of the eigenvector matrix F . The first option is to normalize the eigenvectors to a length of 1. The result of such a normalization is:

$${}^1F = \begin{bmatrix} \sqrt{1/3} & \sqrt{1/2} & 2/3 \\ \sqrt{1/3} & 0 & -1/3 \\ \sqrt{1/3} & -\sqrt{1/2} & 2/3 \end{bmatrix} \quad (15)$$

This normalization is automatically performed by the *eig* function in MATLAB™ [6]. For structural dynamics purposes however it is more meaningful to apply the second option for

normalization using the mass matrix \mathbf{M} for normalization because we will ultimately work in modal coordinates. Normal (= modal) coordinates allow to write an arbitrary motion of the system as a linear combination of the eigenvectors (= modeshapes), since these form an orthogonal set. The modal mass matrix $\tilde{\mathbf{M}}$ is obtained by pre-multiplying \mathbf{M} with the transpose of \mathbf{F} and by post-multiplying with \mathbf{F} .

$$\mathbf{F}^T \mathbf{M} \mathbf{F} = \tilde{\mathbf{M}} = \tilde{\mathbf{M}}^{1/2} \cdot \tilde{\mathbf{M}}^{1/2} \tag{16}$$

Thus the normal modes of an undamped structure are orthogonal by the mass matrix. $\tilde{\mathbf{M}}$ is the matrix containing the modal masses on the main diagonal. We can thus rewrite the right side of equation (16) as shown above. Pre and post-multiplication with $\tilde{\mathbf{M}}^{-1/2}$ yields,

$$\underbrace{(\tilde{\mathbf{M}}^{-1/2})^T}_{\text{}^o\mathbf{F}^T} \underbrace{\mathbf{F}^T \mathbf{M} \mathbf{F}}_{\text{}^o\mathbf{F}} \tilde{\mathbf{M}}^{-1/2} = (\tilde{\mathbf{M}}^{-1/2})^T \tilde{\mathbf{M}}^{1/2} \cdot \tilde{\mathbf{M}}^{1/2} \tilde{\mathbf{M}}^{-1/2} = \mathbf{I} \tag{17}$$

since $(\tilde{\mathbf{M}}^{-1/2})^T = \tilde{\mathbf{M}}^{-1/2}$ we can write

$$\text{}^o\mathbf{F}^T \mathbf{M} \text{}^o\mathbf{F} = \mathbf{I} = \begin{pmatrix} 1 & 0 & 0 \\ 0 & 1 & 0 \\ 0 & 0 & 1 \end{pmatrix} \tag{18}$$

$\text{}^o\mathbf{F}$ is called the mass normalized mode shape matrix. Applying the above derivation to our sample problem we get the following result by substituting in (16):

$$\mathbf{F}^T \mathbf{M} \mathbf{F} = \begin{pmatrix} 1 & 1 & 1 \\ 1 & 0 & -1 \\ 2 & -1 & 2 \end{pmatrix} \begin{pmatrix} m & 0 & 0 \\ 0 & 4m & 0 \\ 0 & 0 & m \end{pmatrix} \begin{pmatrix} 1 & 1 & 2 \\ 0 & -1 & 0 \\ -1 & 2 & 0 \end{pmatrix} = \tilde{\mathbf{M}} = \begin{pmatrix} 6m & 0 & 0 \\ 0 & 2m & 0 \\ 0 & 0 & 12m \end{pmatrix} \tag{19}$$

Thus the modal masses are 1200, 400 and 2400 kg respectively. The mass normalized modeshape matrix is given as:

$${}^o\mathbf{F} = \mathbf{F} \tilde{\mathbf{M}}^{-1/2} = \begin{pmatrix} 1 & 2 & \frac{1}{\sqrt{6m}} & 0 & 0 \\ 0 & -1 & 0 & \frac{1}{\sqrt{2m}} & 0 \\ -1 & 2 & 0 & 0 & \frac{1}{\sqrt{12m}} \end{pmatrix} = \begin{pmatrix} \frac{1}{\sqrt{6m}} & \frac{1}{\sqrt{2m}} & \frac{2}{\sqrt{12m}} \\ \frac{1}{\sqrt{6m}} & 0 & \frac{-1}{\sqrt{12m}} \\ \frac{1}{\sqrt{6m}} & \frac{-1}{\sqrt{2m}} & \frac{2}{\sqrt{12m}} \end{pmatrix} \quad (20)$$

There exists a second useful orthogonality relationship of the mode shape matrix with the stiffness matrix \mathbf{K} . First the matrix of eigenvalues \mathbf{L} is defined as,

$$\mathbf{L} = \mathbf{W}^2 = \begin{pmatrix} w_1^2 & 0 & 0 \\ 0 & w_2^2 & 0 \\ 0 & 0 & w_3^2 \end{pmatrix} = \begin{pmatrix} \mathbf{I}_1 & 0 & 0 \\ 0 & \mathbf{I}_2 & 0 \\ 0 & 0 & \mathbf{I}_3 \end{pmatrix} \quad (21)$$

where pre-multiplication of \mathbf{K} with \mathbf{F}^T and post-multiplication with \mathbf{F} gives,

$$\mathbf{F}^T \mathbf{K} \mathbf{F} = \tilde{\mathbf{M}} \mathbf{L} \quad (22)$$

as with the mass matrix we pre- and post-multiply with $\tilde{\mathbf{M}}^{-1/2}$ and obtain

$$\underbrace{(\tilde{\mathbf{M}}^{-1/2})^T}_{{}^o\mathbf{F}^T} \mathbf{F}^T \mathbf{K} \mathbf{F} \underbrace{\tilde{\mathbf{M}}^{-1/2}}_{{}^o\mathbf{F}} = \mathbf{L} = {}^o\mathbf{F}^T \mathbf{K} {}^o\mathbf{F} = \mathbf{L} = \mathbf{W}^2 \quad (23)$$

We have seen that the set of eigenvectors is a linearly independent, orthogonal set of $N = 3$ vectors and can be used as a basis for the N space. This is closely related to the notion of modal expansion, where an arbitrary motion of the structure can be represented in terms of the modal contributions. We can write the following transformation from physical coordinates to modal coordinates:

$$\mathbf{x} = {}^o\mathbf{F} \mathbf{x} \quad (24)$$

This linear transformation through the mass normalized mode shape matrix ${}^o\mathbf{F}$ can be written componentwise as,

$$\begin{Bmatrix} x_1 \\ x_2 \\ x_3 \end{Bmatrix} = \underbrace{\begin{bmatrix} {}^o f_1 & {}^o f_2 & {}^o f_3 \end{bmatrix}}_{{}^o\mathbf{F}} \begin{Bmatrix} \mathbf{x}_1 \\ \mathbf{x}_2 \\ \mathbf{x}_3 \end{Bmatrix} = {}^o f_1 \mathbf{x}_1 + {}^o f_2 \mathbf{x}_2 + {}^o f_3 \mathbf{x}_3 \quad (25)$$

where the \mathbf{x}_i 's are the modal (also called normal) coordinates. \mathbf{x}_1 for example represents the contribution of mode 1 to the motion of the physical coordinates x_1 , x_2 and x_3 . By substituting (24) in the original equations of motion (3) we obtain the equations of motion in modal space

$$\mathbf{M} \ddot{\mathbf{x}} + \mathbf{K} \mathbf{x} = \mathbf{M} {}^o\mathbf{F} \ddot{\bar{\mathbf{x}}} + \mathbf{K} {}^o\mathbf{F} \bar{\mathbf{x}} = \mathbf{F} \quad (26)$$

and pre-multiplication with ${}^o\mathbf{F}^T$ yields

$$\underbrace{{}^o\mathbf{F}^T \mathbf{M} {}^o\mathbf{F}}_{\mathbf{I}} \ddot{\bar{\mathbf{x}}} + \underbrace{{}^o\mathbf{F}^T \mathbf{K} {}^o\mathbf{F}}_{\mathbf{W}^2} \bar{\mathbf{x}} = \underbrace{{}^o\mathbf{F}^T \mathbf{F}}_{\mathbf{Q}} \quad (27)$$

Invoking the orthogonalities that were derived earlier, we can rewrite the equations of motion as a function of the modal coordinates $\bar{\mathbf{x}}$, the normal frequency matrix \mathbf{W}^2 and the modal force matrix \mathbf{Q} . The matrix \mathbf{Q} represents the effective modal influence of the physical Forces \mathbf{F} .

$$\mathbf{Q} = {}^o\mathbf{F}^T \mathbf{F} \quad (28)$$

The modal force matrix \mathbf{Q} is also closely related to controllability and disturbability. Specifically, if ${}^o\mathbf{F}$ contains a zero at a given degree of freedom (row) and specific mode (column), this means that an applied control input force or disturbance force will have no effect at that location for that particular mode.

The modal form of the equations of motion (27) is especially convenient, because the coupled 2nd order differential equations from (3) are now decoupled, which makes them easy to solve. Now

is also a good time to add damping to the system, since damping (= dissipation of mechanical energy) is always present in physical systems. Since damping is not easy to determine a priori, the modal damping ratios z_i are often determined empirically. The modal damping matrix \mathbf{Z} is diagonal and is given as:

$$\mathbf{Z} = \begin{pmatrix} z_1 & 0 & 0 \\ 0 & z_2 & 0 \\ 0 & 0 & z_3 \end{pmatrix} \quad (29)$$

The modal damping coefficients are often different for every mode in practice and typically vary between 0.1% and 3% for lightly damped space structures [7]. One of the largest uncertainties in spacecraft conceptual design is associated with modal damping. The damping ratios depend on a number of factors such as freeplay, material properties and temperature. For this sample problem we will assume $z_i = 0.005$. The equations of motion in modal coordinates become,

$$\ddot{\mathbf{x}} + 2\mathbf{Z}\mathbf{W}\dot{\mathbf{x}} + \mathbf{W}^2\mathbf{x} = \mathbf{Q} = {}^o\mathbf{F}^T\mathbf{F} \quad (30)$$

if we solve this equation for $\ddot{\mathbf{x}}$ we obtain

$$\ddot{\mathbf{x}} = -2\mathbf{Z}\mathbf{W}\dot{\mathbf{x}} - \mathbf{W}^2\mathbf{x} + {}^o\mathbf{F}^T\mathbf{F} \quad (31)$$

We can write a state vector of modal coordinates and modal velocities as follows,

$$\mathbf{q}_p = \begin{pmatrix} \mathbf{x} \\ \dot{\mathbf{x}} \end{pmatrix} \quad (32)$$

whereby the subscript p indicates that we are dealing with the states of the structural plant. The modal force matrix \mathbf{Q} can be broken up into contributions from control inputs \mathbf{u} and disturbances \mathbf{w} , where \mathbf{b}_u and \mathbf{b}_w are the control and disturbance influence coefficient matrix respectively. \mathbf{b}_u

and \mathbf{b}_w are matrices that usually contain only ones or zeros to indicate at which degrees of freedom of the structural plant the forces act.

$$\mathbf{Q} = {}^o\mathbf{F}^T \mathbf{F} = {}^o\mathbf{F}^T \mathbf{F}_u + {}^o\mathbf{F}^T \mathbf{F}_w = {}^o\mathbf{F}^T \mathbf{b}_u \mathbf{u} + {}^o\mathbf{F}^T \mathbf{b}_w \mathbf{w} \quad (33)$$

with (32) and (33), we can write the equations of motion (the “dynamics”) in 2nd order modal form, while assuming that the structure exhibits linear behavior.

$$\frac{d\dot{\mathbf{q}}_p}{dt} = \underbrace{\begin{bmatrix} \mathbf{0} & \mathbf{I} \\ -\mathbf{W}^2 & -2\mathbf{Z}\mathbf{W} \end{bmatrix}}_{\mathbf{A}_p} \mathbf{q}_p + \underbrace{\begin{bmatrix} \mathbf{0} \\ {}^o\mathbf{F}^T \mathbf{b}_u \end{bmatrix}}_{\mathbf{B}_u} \mathbf{u} + \underbrace{\begin{bmatrix} \mathbf{0} \\ {}^o\mathbf{F}^T \mathbf{b}_w \end{bmatrix}}_{\mathbf{B}_w} \mathbf{w} \quad (34)$$

The other important relationships, that complete the state space representation, are the output \mathbf{y} and the performance \mathbf{z} equation. In general the outputs are given as a linear combination of the coordinates in physical space, or as a combination of states in modal space:

$$\mathbf{y} = \mathbf{C}_{yx} \mathbf{x} + \mathbf{C}_{y\dot{x}} \dot{\mathbf{x}} = \mathbf{C}_{yx} {}^o\mathbf{F} \mathbf{x} + \mathbf{C}_{y\dot{x}} {}^o\mathbf{F} \dot{\mathbf{x}} = \begin{bmatrix} \mathbf{C}_{yx} {}^o\mathbf{F} & \mathbf{C}_{y\dot{x}} {}^o\mathbf{F} \end{bmatrix} \mathbf{q}_p \quad (35)$$

Output equation:
$$\mathbf{y} = \underbrace{\begin{bmatrix} \mathbf{C}_{yx} {}^o\mathbf{F} & \mathbf{C}_{y\dot{x}} {}^o\mathbf{F} \end{bmatrix}}_{\mathbf{C}_y} \mathbf{q}_p + \underbrace{\begin{bmatrix} \mathbf{0} \\ \mathbf{0} \end{bmatrix}}_{\mathbf{D}_{yu}} \mathbf{u} + \underbrace{\begin{bmatrix} \mathbf{0} \\ \mathbf{0} \end{bmatrix}}_{\mathbf{D}_{yw}} \mathbf{w} \quad (36)$$

Performance equation:
$$\mathbf{z} = \underbrace{\begin{bmatrix} \mathbf{C}_{zx} {}^o\mathbf{F} & \mathbf{C}_{z\dot{x}} {}^o\mathbf{F} \end{bmatrix}}_{\mathbf{C}_z} \mathbf{q}_p + \underbrace{\begin{bmatrix} \mathbf{0} \\ \mathbf{0} \end{bmatrix}}_{\mathbf{D}_{zu}} \mathbf{u} + \underbrace{\begin{bmatrix} \mathbf{0} \\ \mathbf{0} \end{bmatrix}}_{\mathbf{D}_{zw}} \mathbf{w} \quad (37)$$

The vector \mathbf{y} contains all the outputs of the system, which are captured by sensors, i.e. they are actually measured, whereas \mathbf{z} contains the metrics by which we will assess the performance of the system. The matrices \mathbf{C}_{yx} , $\mathbf{C}_{y\dot{x}}$ and \mathbf{C}_{zx} , $\mathbf{C}_{z\dot{x}}$ determine the linear combination displacements and rates that contribute to the sensor measurements and performances. It is one of the most demanding tasks of integrated modeling to determine the \mathbf{C} matrices correctly for a specific application. The determination of \mathbf{C}_{yx} , $\mathbf{C}_{y\dot{x}}$ will be covered in the controls modeling section, since it is a controller that ultimately uses the sensor signals. Determination of \mathbf{C}_{zx} , $\mathbf{C}_{z\dot{x}}$ will be

covered in the optics modeling section, since the displacements of the structure affect the positions and orientations of optical elements (e.g. fast steering mirrors, delay lines, beam splitters), which in turn affect the travel of science and metrology light through the system. The **D** terms are also called feedthrough terms since they feed **u** and **w** directly to the output side, while bypassing the system dynamics. Usually the feedthrough terms **D** for the structural plant are zero unless model reduction has been performed. The open loop state space system can be written in the following, very compact form,

$$\begin{bmatrix} \dot{q}_p \\ z \\ y \end{bmatrix} = \begin{bmatrix} \mathbf{A}_p & \mathbf{B}_w & \mathbf{B}_u \\ \mathbf{C}_z & \mathbf{D}_{zw} & \mathbf{D}_{zu} \\ \mathbf{C}_y & \mathbf{D}_{yw} & \mathbf{D}_{yu} \end{bmatrix} \begin{bmatrix} q_p \\ w \\ u \end{bmatrix} \tag{38}$$

A block diagram of the closed loop system including the structural plant dynamics is shown in figure 3.

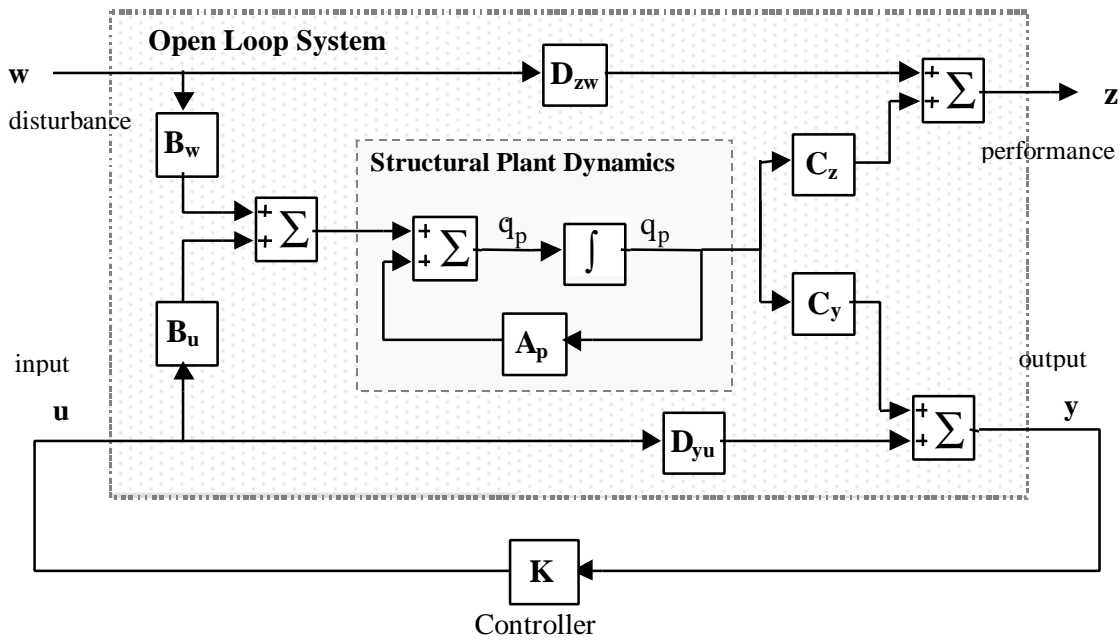


Fig. 3: Block diagram of overall system (D_{yw} and D_{zu} are not shown for simplicity)

It is now time to compute the various matrices of the structural plant for our sample problem. From (34) we can compute the state transition matrix of the structural plant A_p as follows:

$$\mathbf{A}_p = \underbrace{\begin{pmatrix} 0 & I \\ -W^2 & -2ZW \end{pmatrix}}_{\mathbf{A}_p} = \begin{pmatrix} 0 & 0 & 0 & 1 & 0 & 0 \\ 0 & 0 & 0 & 0 & 1 & 0 \\ 0 & 0 & 0 & 0 & 0 & 1 \\ -w_1^2 & 0 & 0 & -2z_1 w_1 & 0 & 0 \\ 0 & -w_2^2 & 0 & 0 & -2z_2 w_2 & 0 \\ 0 & 0 & -w_3^2 & 0 & 0 & -2z_3 w_3 \end{pmatrix} \quad (39a)$$

substituting the previously computed values for the natural frequencies we obtain

$$\mathbf{A}_p = \begin{pmatrix} 0 & 0 & 0 & 1 & 0 & 0 \\ 0 & 0 & 0 & 0 & 1 & 0 \\ 0 & 0 & 0 & 0 & 0 & 1 \\ 0 & 0 & 0 & 0 & 0 & 0 \\ 0 & -\frac{k}{m} & 0 & 0 & -2z_2 \sqrt{\frac{k}{m}} & 0 \\ 0 & 0 & -\frac{3k}{2m} & 0 & 0 & -2z_3 \sqrt{\frac{3k}{2m}} \end{pmatrix} \quad (39b)$$

$$\mathbf{A}_p = \begin{pmatrix} 0 & 0 & 0 & 1 & 0 & 0 \\ 0 & 0 & 0 & 0 & 1 & 0 \\ 0 & 0 & 0 & 0 & 0 & 1 \\ 0 & 0 & 0 & 0 & 0 & 0 \\ 0 & -35500 & 0 & 0 & -1.884 & 0 \\ 0 & 0 & -53250 & 0 & 0 & -2.308 \end{pmatrix} \quad (39c)$$

The numerical values for (39c) are obtained assuming the physical properties from table 1 and a uniform modal damping ratio of $z_i = 0.005$. This result can be compared with the numerical results from MATLAB™ computations in Appendix 2. The determination of the remaining system matrices shown in figure 3 is the objective of the other disciplines of integrated modeling such as disturbance modeling, performance modeling (optics) and control design.

$$\mathbf{B}_w = \begin{bmatrix} \mathbf{0} \\ \mathbf{F}^T \mathbf{b}_w \end{bmatrix} = \begin{bmatrix} \mathbf{0}_{3 \times 1} \\ f_{21} \\ f_{22} \\ f_{23} \end{bmatrix} = \begin{bmatrix} 0 \\ 0 \\ \frac{1}{\sqrt{6m}} \\ 0 \\ \frac{-1}{\sqrt{12m}} \end{bmatrix}^T \quad (41a)$$

Applying the numerical value for m from above we obtain

$$\mathbf{B}_w = [0 \ 0 \ 0 \ .02887 \ 0 \ -0.0204]^T \quad (41b)$$

It is interesting to note that there are only zeros in the two states, which correspond to mode 2, the symmetric mode. This is due to the fact that the central mass is sitting at a node of the structure and this mode is not disturbable. Controllability, disturbability, observability and performability for this system will be investigated more in detail in the integrated modeling section and future memos.

The second step in characterizing the disturbance is to characterize the frequency content of the disturbance energy. Representing the frequency content in power spectral density (PSD) form conveniently does this. In our sample case we assume that the speed distribution of the wheels inside the RWA is uniform and that only the component F_x enters the system at the central mass. The noise energy is thus concentrated over a certain frequency region, whereby the maximum achievable wheel speed determines the cutoff frequency of the disturbance, i.e. the disturbance is band limited. Since higher harmonics are usually present in the disturbance signal, the cutoff frequency doesn't necessarily correspond to the fundamental frequency of wheel rotation. A convenient way off thinking of this problem is to imagine a source of white noise, which is filtered by a "disturbance" transfer function.

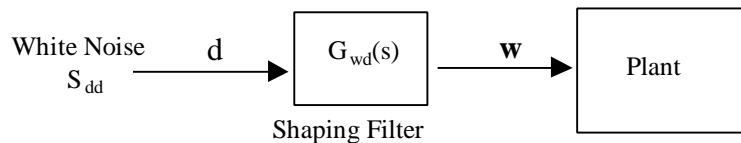


Fig. 4: Representation of disturbance with shaping filter

The simplest such transfer function is a low-pass filter (LPF) of the form

$${}^{LPF}G_{wd}(s) = \frac{w(s)}{d(s)} = \frac{\omega_{RO}}{s + \omega_{RO}} \quad (42)$$

where $w(s)$ is the shaped disturbance, $d(s) = 1$ is the white noise, $s = j\omega$ is the complex frequency and ω_{RO} is the rolloff or corner frequency in rad/sec. The disturbance power spectral density (PSD) function can be obtained from the following relationship [8] as,

$$S_{ww}(\omega) = G_{wd}(j\omega) \cdot S_{dd} \cdot G_{wd}(j\omega)^H \quad (43)$$

where S_{dd} is the intensity of the white noise, $G_{wd}(j\omega)$ is the white noise to disturbance transfer function matrix and S_{ww} is the cross spectral density matrix of the disturbance w . For the low-pass filter approximation we obtain:

$${}^{LPF}S_{ww}(\omega) = \frac{S_{dd} \omega_{RO}^2}{\omega^2 + \omega_{RO}^2} = S_{ww}(2\mathbf{f}) = \frac{S_{dd} f_{RO}^2}{f^2 + f_{RO}^2} \quad (44)$$

It shall be noted that the units of the PSD are $N^2/(\text{rad/sec})$ for force disturbances and $(\text{Nm})^2/(\text{rad/sec})$ for moment disturbances. The above relationship only holds true if we assume that the RPM distribution for the wheels varies between 0 and a maximum value. The LPF also significantly overpredicts the energy content at low frequency, since the RWA disturbances scale with the square of the wheel speed. For a variation of RPM, where the lower limit is not zero it is better to use a band-pass filter (BPF) as disturbance shaping filter. The shaping filter for a band-limited noise source is given as

$${}^{BPF}G_{wd}(s) = \frac{w(s)}{d(s)} = \frac{\omega_{RO} s}{(s + \omega_{RU})(s + \omega_{RO})} \quad (45)$$

and the corresponding PSD is

$${}^{BPF} S_{ww}(\mathbf{w}) = \frac{S_{dd} \mathbf{w}_{RO}^2 \mathbf{w}^2}{(\mathbf{w}_{RO}^2 + \mathbf{w}^2)(\mathbf{w}_{RU}^2 + \mathbf{w}^2)} = S_{ww}(2\mathbf{f}) = \frac{S_{dd} f_{RO}^2 f^2}{(f_{RO}^2 + f^2)(f_{RU}^2 + f^2)} \quad (46)$$

In the sample problem we chose $f_{RO} = 100$ Hz and $f_{RU} = 1$ Hz so that $\omega_{RO} = 2\pi f_{RO} = 200\pi$ rad/sec and $\omega_{RU} = 2\pi f_{RU} = 2\pi$ rad/sec. Figure 5 plots the two power spectral densities for the disturbance F_x in the sample problem. As we will see later there are different methods to propagate this disturbance through the system in order to predict the performance z . The frequency domain approach demands PSD's in the form of equations (44) and (46) respectively. The Lyapunov approach however requires that the disturbance filter be written in state space form. Rewriting the LPF transfer function and denoting it as disturbance source 1 we obtain the following:

$${}^{LPF} G_{wd}(s) = \frac{\mathbf{w}_{RO}}{s + \mathbf{w}_{RO}} \quad (47)$$

This can be written in canonical controller form as,

$$\begin{aligned} \dot{q}_{d1} &= [-\mathbf{w}_{RO}]q_{d1} + [1]d = A_{d1}q_{d1} + B_{d1}d \\ w &= [\mathbf{w}_{RO}]q_{d1} + [0]d = C_{d1}q_{d1} + D_{d1}d \end{aligned} \quad (48a)$$

with $\omega_{RO} = 200\pi$ rad/sec we get the following numerical values:

$$\begin{aligned} \dot{q}_{d1} &= [-628.3]q_{d1} + [1]d = A_{d1}q_{d1} + B_{d1}d \\ w &= [628.3]q_{d1} + [0]d = C_{d1}q_{d1} + D_{d1}d \end{aligned} \quad (48b)$$

We only need one state to describe the LPF approximation in state space. Since the BPF contains a second order denominator, we will need 2 states for its state space representation. Again applying the controller canonical form [9] and denoting the BPF as disturbance source 2 results in:

$$\dot{\mathbf{q}}_{d2} = \underbrace{\begin{bmatrix} 0 & 1 \\ -\mathbf{w}_{RU} \mathbf{w}_{RO} & -\mathbf{w}_{RU} - \mathbf{w}_{RO} \end{bmatrix}}_{\mathbf{A}_{d2}} \mathbf{q}_{d2} + \underbrace{\begin{bmatrix} 0 \\ 1 \end{bmatrix}}_{\mathbf{B}_{d2}} d$$

$$w = \underbrace{\begin{bmatrix} 0 & \mathbf{w}_{RO} \end{bmatrix}}_{\mathbf{C}_{d2}} \mathbf{q}_{d2} + \underbrace{\begin{bmatrix} 0 \end{bmatrix}}_{\mathbf{D}_{d2}} d$$
(49a)

this is evaluated to be

$$\dot{\mathbf{q}}_{d2} = \underbrace{\begin{bmatrix} 0 & 1 \\ -3947.8 & -634.5 \end{bmatrix}}_{\mathbf{A}_{d2}} \mathbf{q}_{d2} + \underbrace{\begin{bmatrix} 0 \\ 1 \end{bmatrix}}_{\mathbf{B}_{d2}} d$$

$$w = \underbrace{\begin{bmatrix} 0 & 628.3 \end{bmatrix}}_{\mathbf{C}_{d2}} \mathbf{q}_{d2} + \underbrace{\begin{bmatrix} 0 \end{bmatrix}}_{\mathbf{D}_{d2}} d$$
(49b)

This is the disturbance representation of the band-pass filter in state space form. For this analysis we will assume unit intensity white noise so that $S_{dd}=1$. The feedthrough terms \mathbf{D}_{zw} and \mathbf{D}_{yw} are zero. Figure 5 shows a comparison of the LPF (left) and BPF (right) disturbance PSD's.

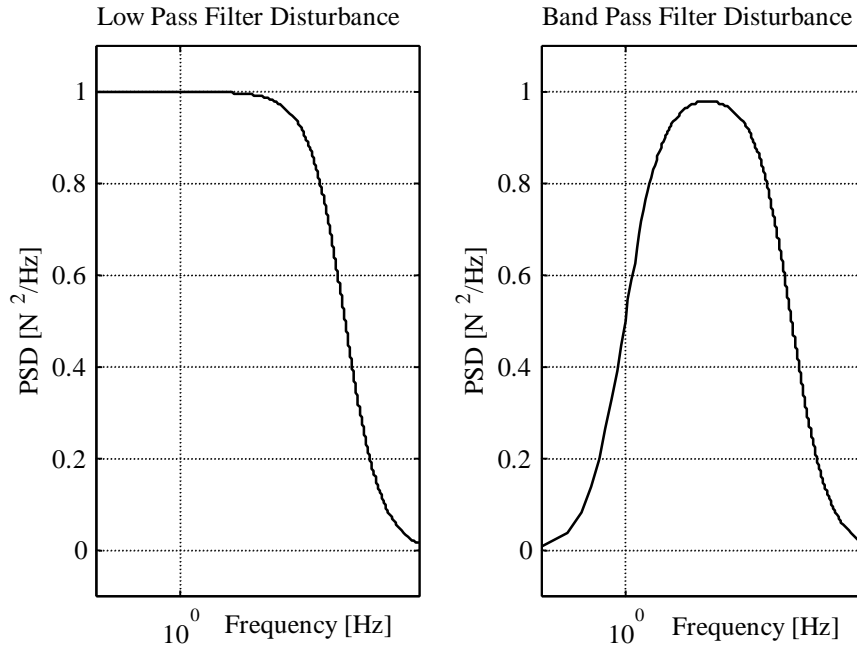


Fig. 5: Comparison of LPF and HPF disturbance shaping filters

4. Optics – Performance Modeling

Of all the tasks in the integrated modeling process the accurate modeling of the performance metrics is one of the most important and challenging tasks. For space and ground based observatories these metrics have to be derived from geometrical ray tracing, or if diffraction effects are of importance, Fourier optics has to be invoked. In principal the task involves first designing the optical train, i.e. the path and elements which collect and process the science and guidance light beams from the first collector to the detectors in the instrument module. Typical elements on the optical path are conical and flat fixed mirrors, deformable mirrors, fast steering mirrors, beam compressors, refractive lenses, beam splitters and combiners, polarization filters, optical delay lines and the detectors themselves. The next step consists in developing an optical prescription for each of these elements, which produces the final desired result. After that the optical elements have to be placed on the structure at appropriate locations. The most difficult step is to derive the actual performance metrics and their functional dependency on the structural degrees of freedom. Significant progress in this area was achieved by Redding and co-workers [13].

Our sample problem shall illustrate this process in a simplified manner. The first step consists in performing a ray trace of the science light through the system. For the sample example the science light is collected at the apertures and then redirected toward the central mass, where it is interfered. The details of beam compressors, mirrors and optical delay lines (ODL's) are not modeled for this simple example. Figure 6 shows the two pathlengths of the light OPL1 and OPL2.

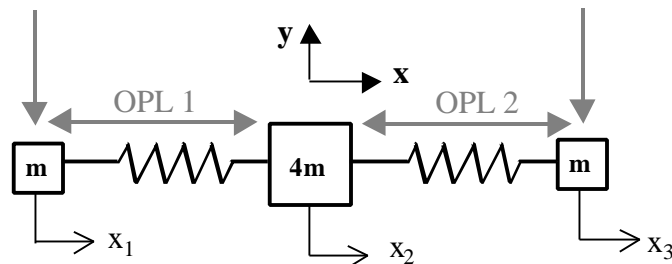


Fig.6: Ray Trace for sample 3-DOF problem

We choose the optical pathlength difference (OPD) as the performance metric, i.e. the optical pathlength difference is the difference in the distance between the left aperture and the right aperture from the central mass. This can be computed as:

$$OPD = OPL_1 - OPL_2 \tag{50}$$

The pathlengths OPL1 and OPL2 are given as

$$\begin{aligned} OPL_1 &= l_0 + (x_2 - x_1) \\ OPL_2 &= l_0 + (x_3 - x_2) \end{aligned} \tag{51}$$

computing the OPD from (50) gives

$$OPD = OPL_1 - OPL_2 = l_0 + x_2 - x_1 - l_0 - x_3 + x_2 = -x_1 + 2x_2 - x_3 \tag{52}$$

and in matrix form

$$z = OPD = \underbrace{\begin{bmatrix} -1 & 2 & -1 \end{bmatrix}}_{\mathbf{C}_{zx}} \begin{bmatrix} x_1 \\ x_2 \\ x_3 \end{bmatrix} \tag{53}$$

The matrix \mathbf{C}_{zx} is also called the optics linear sensitivity matrix since it relates the physical displacements of the structure to the optical performance metrics of interest. A number of simplifications have been made here since the OPD only accounts for internal pathlength differences. If rotations and y-displacements were allowed in the problem, we could also include the external OPD, which is due to a rigid body rotation of the entire spacecraft. This external difference is measured with respect to a reference plane of the incoming planar stellar wavefront.

At this point it is also necessary to establish a performance requirement. Typically engineering requirements are levied as a 1σ (= RMS if zero mean) requirement. For diffraction limited performance at a given wavelength λ , the OPD is constrained to be smaller than [11]

$$OPD \leq \frac{\lambda}{20} \quad (54a)$$

Since we never want to exceed this upper bound, but we are dealing with random stochastic vibration processes, we will treat $\lambda/20$ as a 3σ upper bound, so that the following requirement for the OPD_{RMS} emerges:

$$s_{OPD} = OPD_{RMS} \leq \frac{\lambda}{60} \quad (54b)$$

For the sample problem we will assume a wavelength of $\lambda = 7 \mu\text{m} = 7000 \text{ nm}$ in the IR portion of the electromagnetic spectrum, so that the OPD_{RMS} must be $\leq 116 \text{ nm}$. For observatories working in the near IR, visual or UV regimes the requirements are tighter due to the shorter wavelength.

According to (37) we have to compute the performance C matrix \mathbf{C}_z in modal space using the linear sensitivity matrix \mathbf{C}_{zx} we derived above. We have only displacement and no rate dependency for the OPD.

$$\mathbf{C}_z = [\mathbf{C}_{zx}^o \mathbf{F} \quad \mathbf{C}_{zx}^o \mathbf{F}] = [\mathbf{C}_{zx}^o \mathbf{F} \quad \mathbf{0}] \quad (55)$$

Assuming we want to obtain the performance (OPD) in units of nanometers (10^{-9} m), we incorporate a scale factor $s_c = 1 \cdot 10^9$ into the \mathbf{C}_z matrix, which is computed as follows:

$$\mathbf{C}_{\mathbf{z}\mathbf{x}}^o \mathbf{F} = \begin{bmatrix} -1 & 2 & -1 \end{bmatrix} \begin{bmatrix} \frac{1}{\sqrt{6m}} & \frac{1}{\sqrt{2m}} & \frac{2}{\sqrt{12m}} \\ \frac{1}{\sqrt{6m}} & 0 & \frac{-1}{\sqrt{12m}} \\ \frac{1}{\sqrt{6m}} & \frac{-1}{\sqrt{2m}} & \frac{2}{\sqrt{12m}} \end{bmatrix} = \begin{bmatrix} 0 & 0 & \frac{-6}{\sqrt{12m}} \end{bmatrix} \quad (56)$$

thus the performance matrix is given as

$$\mathbf{C}_{\mathbf{z}} = \begin{bmatrix} s_c \mathbf{C}_{\mathbf{z}\mathbf{x}}^o \mathbf{F} & \mathbf{0} \end{bmatrix} = \begin{bmatrix} 0 & 0 & -6s_c/\sqrt{12m} & 0 & 0 & 0 \end{bmatrix} \quad (57a)$$

$$\mathbf{C}_{\mathbf{z}} = \begin{bmatrix} s_c \mathbf{C}_{\mathbf{z}\mathbf{x}}^o \mathbf{F} & \mathbf{0} \end{bmatrix} = \begin{bmatrix} 0 & 0 & -1.22e8 & 0 & 0 & 0 \end{bmatrix} \quad (57b)$$

It is interesting to note that the only non-zero entry in $\mathbf{C}_{\mathbf{z}}$ is related to the third mode. This indicates that mode 1 and mode 2 do not contribute to the OPD. Indeed this is reasonable when we consult the modeshapes on figure 4. In the rigid body mode (mode 1) all masses move by the same amount simultaneously and no differential pathlength is created. In the second mode both masses move symmetrically with respect to the combiner location. Even though the optical pathlength is changing, the *difference* between the two paths is still zero for the second mode. Only the third mode contributes, since the masses move by different amounts, thus creating a non-zero optical pathlength difference. The feedthrough terms $\mathbf{D}_{\mathbf{z}\mathbf{w}}$ and $\mathbf{D}_{\mathbf{z}\mathbf{u}}$ are zero.

5. Control Design

The last step before assembling the integrated model consists in designing a control system, which is often responsible for bringing the optical performance within the bounds set by the requirements. Due to these stringent requirements it is reasonable to predict that all future space science missions will incorporate control systems not only at the ACS level, but also for optical control. Traditionally the attitude determination and control system (ADCS) is designed to stabilize the rigid body modes of the spacecraft. In order to ensure sufficient stability margins the bandwidth of the ACS is often set to be about 1 decade below the first flexible mode of the structure. The second control system that is often modeled, as a decoupled system from the ACS, is optical control. Depending on the application the optical control incorporates deformable

sensor. In other words it maps the structural states into the ideal sensor measurements. The matrix \mathbf{C}_y is closely related to the notion of observability. The matrix \mathbf{B}_u maps the control inputs into forces and moments at the appropriate degrees of freedom of the structural model.

Optical Control: For the sample problem a laser metrology system is used as a sensor that gives a measure of the actual pathlength difference between the two collectors. It is assumed that the bandwidth, dynamic range, resolution and accuracy of the laser metrology system are sufficient for this application. The laser metrology system consists of two laser interferometers, which are located on the central mass. They bounce off a laser beam from a mirror, which is mounted, on each aperture and measure the traveled distance (which corresponds to twice the OPL for each arm). The sensor output y is then the difference between the two laser measurements.

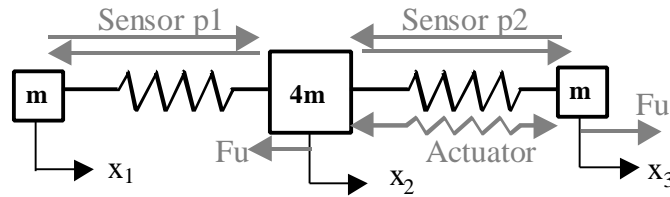


Fig. 8: DPL measurement with laser metrology system

$$\begin{aligned} p_1 &= 2l_0 + x_2 - x_1 \\ p_2 &= 2l_0 + x_3 - x_2 \end{aligned} \quad (58)$$

the sensor output is given as

$$y = p_2 - p_1 = 2x_3 - 4x_2 + 2x_1 \quad (59)$$

In matrix form we obtain the output (ideal sensor measurement) as written in the following equation. It is assumed that the sensor is high quality and is able to amplify the signal, such that the sensor output is in units of nm, therefore a scale factor $s_c = 1 \cdot 10^9$ is included in the \mathbf{C}_y matrix

$$y = s_c \cdot \underbrace{\begin{bmatrix} 2 & -4 & 2 \end{bmatrix}}_{\mathbf{C}_{yx}} \begin{bmatrix} x_1 \\ x_2 \\ x_3 \end{bmatrix} \quad (60)$$

The following relationship exists between \mathbf{C}_{yx} and \mathbf{C}_{zx}

$$\mathbf{C}_{yx} = -2\mathbf{C}_{zx} \quad (61a)$$

the output matrix \mathbf{C}_y is computed assuming that $\mathbf{C}_{yx} = 0$ and ensuring that the output is in nm,

$$\mathbf{C}_y = [s_c \mathbf{C}_{yx} \text{ } ^o\text{F} \text{ } 0] = [0 \text{ } 0 \text{ } s_c \sqrt{12/m} \text{ } 0 \text{ } 0 \text{ } 0] = [0 \text{ } 0 \text{ } 2.449e8 \text{ } 0 \text{ } 0 \text{ } 0] \quad (61b)$$

Ideally for such an application we would use an optical delay line (ODL) for optical control. To simplify matters in the sample problem we assume that we are using a low impedance force actuator, such as an active strut, as represented in figure 8. This actuator commands a differential force rather than differential displacement. The objective of the controller is to bring the OPD to zero, therefore only one of the interferometer arms needs to be equipped with the actuator. Due to “actio=reactio” the actuator exerts a force F_u of equal magnitude but opposite sign on nodes 2 and 3. Thus we can write

$$\mathbf{u} = \begin{bmatrix} 0 \\ -F_u \\ F_u \end{bmatrix} = \underbrace{\begin{bmatrix} 0 & -1 & 1 \end{bmatrix}^T}_{\mathbf{b}_u} F_u \quad (62)$$

the matrix \mathbf{B}_u is obtained in an analog fashion as \mathbf{C}_y :

$$\mathbf{B}_u = \begin{bmatrix} 0 \\ F_u^T \mathbf{b}_u \end{bmatrix} \quad (63)$$

the lower half of \mathbf{B}_u is

$${}^o\mathbf{F}^T \mathbf{b}_u = \begin{bmatrix} \frac{1}{\sqrt{6m}} & \frac{1}{\sqrt{6m}} & \frac{1}{\sqrt{6m}} \\ 1 & 0 & -1 \\ \frac{1}{\sqrt{2m}} & 0 & \frac{1}{\sqrt{2m}} \\ 2 & -1 & 2 \\ \frac{1}{\sqrt{12m}} & \frac{1}{\sqrt{12m}} & \frac{1}{\sqrt{12m}} \end{bmatrix} \begin{bmatrix} 0 \\ -1 \\ 1 \end{bmatrix} = \begin{bmatrix} 0 \\ -1 \\ \frac{1}{\sqrt{2m}} \\ 3 \\ \frac{1}{\sqrt{12m}} \end{bmatrix} \quad (64)$$

thus the input influence matrix \mathbf{B}_u is

$$\mathbf{B}_u = \begin{bmatrix} 0 & 0 & 0 & 0 & -1/\sqrt{2m} & 3/\sqrt{12m} \\ 0 & 0 & 0 & 0 & -0.05 & 0.0612 \end{bmatrix}^T \quad (65)$$

Since there is no feedthrough from u to y , we can set the feedthrough term \mathbf{D}_{yu} to zero. The controller will be a SISO controller, which receives the y measurement from the laser metrology system and issues a force command u to the force actuator. As a simple solution we choose a PD-controller with time delay and use classical control techniques to design and analyze it. We thus apply static compensation of the OPD and provide rate feedback. The feedback equation is:

$$u = -\mathbf{K} y \quad (66)$$

For PD control with negative feedback and time delay we write

$$K(s) = K_p + \frac{K_d s}{\tau_d s + 1} \quad (67)$$

where K_p is the proportional gain, K_d is the derivative gain and τ_d is the time delay [10]. The controller transfer function can be rewritten as:

$$K(s) = \frac{u(s)}{y(s)} = \frac{(K_p \tau_d + K_d) s + K_p}{\tau_d s + 1} = \frac{a_1 s + a_0}{b_1 s + b_0} \quad (68)$$

The controller canonical form³ of the controller transfer function is given as

$$\begin{aligned}\frac{dq_c}{dt} &= \left[\frac{-b_o}{b_1} \right] q_c + [1] y \\ u &= \left[\frac{a_o b_1 - a_1 b_o}{b_1^2} \right] q_c + \left[\frac{a_1}{b_1} \right] y\end{aligned}\tag{69}$$

Substituting the coefficients obtained by comparison of (68) and (69) we obtain the controller state space representation

$$\begin{aligned}\frac{d\dot{q}_c}{dt} &= \underbrace{\left[-1/\mathbf{t}_d \right]}_{\mathbf{A}_c} q_c + \underbrace{\left[1 \right]}_{\mathbf{B}_c} y \\ u &= \underbrace{\left[-K_d/\mathbf{t}_d^2 \right]}_{\mathbf{C}_c} q_c + \underbrace{\left[K_p + K_d/\mathbf{t}_d \right]}_{\mathbf{D}_c} y\end{aligned}\tag{70}$$

After some initial trials we chose $K_p=0.01$ and $K_d=0.05$ as initial controller gain values. This assumes that the sensor signal is provided in units of nm. It will be the goal of the performance improvement section (part 4) to tune these parameters. The time delay is expected to be $\tau_d = 0.1$ sec.

ACS: This is also the point where a full attitude determination and control system design should take place. This is required in order to stabilize the rigid body mode. Instead of modeling the ACS in detail we represent the effect of a closed loop ACS by stiffening and dampening the rigid body mode. The plant dynamics matrix \mathbf{A}_p is ill conditioned in the present state. The condition number c_{A_p} is given as the ratio of the largest singular value of \mathbf{A}_p to the smallest singular value:

³ This definition is also compatible with the MATLAB tf2ss.m function

$$c_{A_p} = \frac{\mathbf{s}_{A_p}^{\max}}{\mathbf{s}_{A_p}^{\min}} = 2.53 \cdot 10^{16} \tag{71a}$$

A large condition number indicates that \mathbf{A}_p is nearly singular. Assuming a 1 Hz bandwidth of the ACS controller and critical damping we set:

$$w_1 = 2\mathbf{p} \left(\frac{\text{rad}}{\text{sec}} \right), \quad z_1 = .707 \tag{72}$$

so that the \mathbf{A}_p matrix with the stabilized rigid body mode looks as follows:

$$\mathbf{A}_p = \begin{pmatrix} 0 & 0 & 0 & 1 & 0 & 0 \\ 0 & 0 & 0 & 0 & 1 & 0 \\ 0 & 0 & 0 & 0 & 0 & 1 \\ -39.47 & 0 & 0 & -8.8844 & 0 & 0 \\ 0 & -35500 & 0 & 0 & -1.884 & 0 \\ 0 & 0 & -53250 & 0 & 0 & -2.308 \end{pmatrix} \tag{73}$$

The condition number of the stabilized \mathbf{A}_p matrix is now significantly lower

$$c_{A_p} = \frac{\mathbf{s}_{A_p}^{\max}}{\mathbf{s}_{A_p}^{\min}} = 5.4583 \cdot 10^4 \tag{71b}$$

At this point we need to assemble and analyze the performance and stability of the closed loop system. This is done in the integrated modeling section.

6. Integrated Modeling

The main task of integrated modeling is to assemble the results from the previous sections, i.e. structural, disturbance, performance and controls models into one overall model. For linear systems this model is usually represented in state space form. Additionally the integrated

modeler needs to analyze the closed loop system for stability, observability and controllability to ensure that no mistakes have been made previously and that the system is well conditioned for subsequent analysis. The Lyapunov analysis for example requires that the system be stable, e.g. the A_{zd} matrix must be non-singular. It is thus paramount that the rigid body modes of the system have either been removed or stabilized by the ACS.

For the Lyapunov analysis it is desirable to integrate the disturbance, structural and controls models together into one system. This system describes the dynamics from a white noise source input d to the performance metrics z . The first step is to append the disturbance states q_d , the structural plant states q_p and the control states q_c into an overall state vector:

$$q = \begin{bmatrix} q_d \\ q_p \\ q_c \end{bmatrix} \tag{74}$$

The overall system dynamics are then written by appending the system together according to the following block diagram:

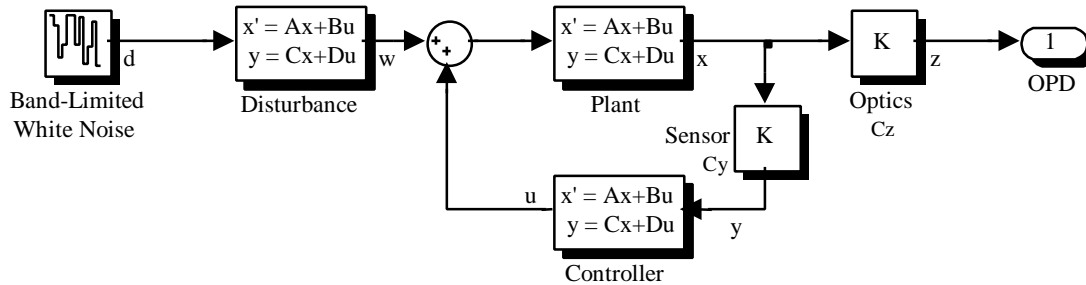


Fig. 9: Integrated model for 3DOF sample problem

Going from left to right we can write the individual state equations and append them together. The disturbance model from equation (48) is given as :

$$\begin{aligned} \dot{q}_d &= A_d q_d + B_d d \\ w &= C_d q_d \end{aligned} \tag{75}$$

The feedthrough term \mathbf{D}_a has to be set to zero, since we cannot allow the white noise disturbance to pass through the system due to its infinite variance. The plant state equation and the performance and output equations from (34) are

$$\begin{aligned} \dot{\mathbf{q}}_p &= \mathbf{A}_p \mathbf{q}_p + \mathbf{B}_u u + \mathbf{B}_w w \\ y &= \mathbf{C}_y \mathbf{q}_p \\ z &= \mathbf{C}_z \mathbf{q}_p \end{aligned} \tag{76}$$

and the controller state equations from (70) are given as

$$\begin{aligned} \frac{dq_c}{dt} &= \mathbf{A}_c q_c + \mathbf{B}_c y \\ u &= \mathbf{C}_c q_c + \mathbf{D}_c y \end{aligned} \tag{77}$$

Obviously here we cannot set the controller feedthrough term \mathbf{D}_c to zero, since it is not zero due to the use of proportional feedback. The plant and controller states can now be rewritten as:

$$\begin{aligned} \dot{\mathbf{q}}_p &= \mathbf{A}_p \mathbf{q}_p + \mathbf{B}_u \mathbf{C}_c q_c + \mathbf{B}_u \mathbf{D}_c \mathbf{C}_y \mathbf{q}_p + \mathbf{B}_w \mathbf{C}_d q_d \\ \mathbf{q}_c &= \mathbf{A}_c q_c + \mathbf{B}_c \mathbf{C}_y \mathbf{q}_p \end{aligned} \tag{78}$$

There are therefore four systems we can write, depending if we look at the open loop versus closed loop system and whether we append the disturbance filter into the state equations or not. Table 2 shows the four possibilities in an overview.

State Space Representations	open loop (u = 0)	closed loop (u = -Ky)
disturbance \mathbf{q}_d states excluded	1: SYS_ozw	3:SYS_czw
disturbance \mathbf{q}_d states included	2:SYS_ozd	4:SYS_czd

Table 2: Possibilities for assembling the integrated state space model

The four systems are given as follows:

$$\begin{aligned}
 \begin{bmatrix} \dot{\mathbf{q}}_p \end{bmatrix} &= \begin{bmatrix} \mathbf{A}_p \end{bmatrix} \mathbf{q}_p + \begin{bmatrix} \mathbf{B}_w \end{bmatrix} w \\
 &\quad \mathbf{A}_{ozw} \quad \mathbf{B}_{ozw} \\
 1) \text{ SYS}_{ozw}: \quad z &= \begin{bmatrix} \mathbf{C}_z \end{bmatrix} \mathbf{q}_p + \begin{bmatrix} \mathbf{D}_{zw} \end{bmatrix} w \\
 &\quad \mathbf{C}_{ozw} \quad \mathbf{D}_{ozw}
 \end{aligned} \tag{79}$$

$$\begin{aligned}
 \begin{bmatrix} \dot{\mathbf{q}}_d \\ \dot{\mathbf{q}}_p \end{bmatrix} &= \underbrace{\begin{bmatrix} \mathbf{A}_d & \mathbf{0} \\ \mathbf{B}_w \mathbf{C}_d & \mathbf{A}_p \end{bmatrix}}_{\mathbf{A}_{ozd}} \begin{bmatrix} \mathbf{q}_d \\ \mathbf{q}_p \end{bmatrix} + \underbrace{\begin{bmatrix} \mathbf{B}_d \\ \mathbf{0} \end{bmatrix}}_{\mathbf{B}_{ozd}} d \\
 2) \text{ SYS}_{ozd} \quad z &= \underbrace{\begin{bmatrix} \mathbf{0} & \mathbf{C}_z \end{bmatrix}}_{\mathbf{C}_{ozd}} \begin{bmatrix} \mathbf{q}_d \\ \mathbf{q}_p \end{bmatrix} + \underbrace{\begin{bmatrix} \mathbf{0} \end{bmatrix}}_{\mathbf{D}_{ozd}} d
 \end{aligned} \tag{80}$$

$$\begin{aligned}
 \begin{bmatrix} \dot{\mathbf{q}}_p \\ \dot{\mathbf{q}}_c \end{bmatrix} &= \underbrace{\begin{bmatrix} \mathbf{A}_p + \mathbf{B}_u \mathbf{D}_c \mathbf{C}_y & \mathbf{B}_u \mathbf{C}_c \\ \mathbf{B}_c \mathbf{C}_y & \mathbf{A}_c \end{bmatrix}}_{\mathbf{A}_{czw}} \begin{bmatrix} \mathbf{q}_p \\ \mathbf{q}_c \end{bmatrix} + \underbrace{\begin{bmatrix} \mathbf{B}_w \\ \mathbf{0} \end{bmatrix}}_{\mathbf{B}_{czw}} w \\
 3) \text{ SYS}_{czw} \quad z &= \underbrace{\begin{bmatrix} \mathbf{C}_z & \mathbf{0} \end{bmatrix}}_{\mathbf{C}_{czw}} \begin{bmatrix} \mathbf{q}_p \\ \mathbf{q}_c \end{bmatrix} + \underbrace{\begin{bmatrix} \mathbf{0} \end{bmatrix}}_{\mathbf{D}_{czw}} w
 \end{aligned} \tag{81}$$

$$\begin{aligned}
 \begin{bmatrix} \dot{\mathbf{q}}_d \\ \dot{\mathbf{q}}_p \\ \dot{\mathbf{q}}_c \end{bmatrix} &= \underbrace{\begin{bmatrix} \mathbf{A}_d & \mathbf{0} & \mathbf{0} \\ \mathbf{B}_w \mathbf{C}_d & \mathbf{A}_p + \mathbf{B}_u \mathbf{D}_c \mathbf{C}_y & \mathbf{B}_u \mathbf{C}_c \\ \mathbf{0} & \mathbf{B}_c \mathbf{C}_y & \mathbf{A}_c \end{bmatrix}}_{\mathbf{A}_{czd}} \begin{bmatrix} \mathbf{q}_d \\ \mathbf{q}_p \\ \mathbf{q}_c \end{bmatrix} + \underbrace{\begin{bmatrix} \mathbf{B}_d \\ \mathbf{0} \\ \mathbf{0} \end{bmatrix}}_{\mathbf{B}_{czd}} d \\
 4) \text{ SYS}_{czd} \quad z &= \underbrace{\begin{bmatrix} \mathbf{0} & \mathbf{C}_z & \mathbf{0} \end{bmatrix}}_{\mathbf{C}_{czd}} \begin{bmatrix} \mathbf{q}_d & \mathbf{q}_p & \mathbf{q}_c \end{bmatrix}^T + \underbrace{\begin{bmatrix} \mathbf{0} \end{bmatrix}}_{\mathbf{D}_{czd}} d
 \end{aligned} \tag{82}$$

Since we are dealing with a SISO system it is useful and instructive to analytically compute the transfer functions of the above system. This will be helpful in analytically computing the system performance. The open loop transfer function $G_{ozw}(s)$ can be computed based on the following relationship [9]:

$$G_{ozw}(s) = C_z [sI - A_p]^{-1} B_w + D_{zw} \tag{83}$$

The most time consuming step in computing the transfer function is the matrix inversion involving A_p . In our case, where the system is in modal form we can simplify this step in the analytical calculation by bringing the A_p matrix into Gauss-Jordan form, i.e. it will contain decoupled sub-blocks, which will contain the 2nd order dynamics for each mode.

$$\bar{A}_p = \begin{matrix} \left[\begin{array}{cc|cc} 0 & 1 & 0_{2 \times 2} & 0_{2 \times 2} \\ -w_1^2 & -2z_1 w_1 & 0_{2 \times 2} & 0_{2 \times 2} \end{array} \right] & & & \\ & \left[\begin{array}{cc|cc} 0 & 1 & 0_{2 \times 2} & 0_{2 \times 2} \\ -w_2^2 & -2z_2 w_2 & 0_{2 \times 2} & 0_{2 \times 2} \end{array} \right] & & \\ & & \left[\begin{array}{cc|cc} 0 & 1 & 0_{2 \times 2} & 0_{2 \times 2} \\ -w_3^2 & -2z_3 w_3 & 0_{2 \times 2} & 0_{2 \times 2} \end{array} \right] & & \end{matrix} \tag{84}$$

The following matrix inversion has to be executed analytically, substituting $\omega_1=0$ we get equation (85):

$$[sI - \bar{A}_p]^{-1} = \begin{matrix} \left[\begin{array}{cc|cc} s & -1 & 0_{2 \times 2} & 0_{2 \times 2} \\ 0 & s & 0_{2 \times 2} & 0_{2 \times 2} \end{array} \right]^{-1} & & & \\ & \left[\begin{array}{cc|cc} s & -1 & 0_{2 \times 2} & 0_{2 \times 2} \\ w_2^2 & s + 2z_2 w_2 & 0_{2 \times 2} & 0_{2 \times 2} \end{array} \right]^{-1} & & \\ & & \left[\begin{array}{cc|cc} s & -1 & 0_{2 \times 2} & 0_{2 \times 2} \\ w_3^2 & s + 2z_3 w_3 & 0_{2 \times 2} & 0_{2 \times 2} \end{array} \right]^{-1} & & \end{matrix}$$

$$= \begin{matrix} \left[\begin{array}{cc|cc} 1/s & 1/s^2 & 0_{2 \times 2} & 0_{2 \times 2} \\ 0 & 1/s & 0_{2 \times 2} & 0_{2 \times 2} \end{array} \right] & & & \\ & \left[\begin{array}{cc|cc} \frac{s + 2z_2 w_2}{s^2 + 2z_2 w_2 + w_2^2} & \frac{1}{s^2 + 2z_2 w_2 + w_2^2} & 0_{2 \times 2} & 0_{2 \times 2} \\ \frac{-w_2^2}{s^2 + 2z_2 w_2 + w_2^2} & \frac{s}{s^2 + 2z_2 w_2 + w_2^2} & 0_{2 \times 2} & 0_{2 \times 2} \end{array} \right] & & \\ & & \left[\begin{array}{cc|cc} \frac{s + 2z_3 w_3}{s^2 + 2z_3 w_3 + w_3^2} & \frac{1}{s^2 + 2z_3 w_3 + w_3^2} & 0_{2 \times 2} & 0_{2 \times 2} \\ \frac{-w_3^2}{s^2 + 2z_3 w_3 + w_3^2} & \frac{s}{s^2 + 2z_3 w_3 + w_3^2} & 0_{2 \times 2} & 0_{2 \times 2} \end{array} \right] & & \end{matrix}$$

It is important that the other matrices also have to be reordered according to the Gauss-Jordan formulation. The other matrices to be multiplied with (85) according to (83) are given as

$$\bar{\mathbf{C}}_z = \begin{pmatrix} 0 & 0 & 0 & 0 & \frac{-6s_c}{\sqrt{12m}} & 0 \end{pmatrix} \quad (86)$$

$$\bar{\mathbf{B}}_w = \begin{pmatrix} 0 & \frac{1}{\sqrt{6m}} & 0 & 0 & 0 & \frac{-1}{\sqrt{12m}} \end{pmatrix}^T \quad (87)$$

Since the feed through term \mathbf{D}_{zw} is zero, we can compute the closed form of the open loop transfer function by matrix multiplication. This yields the following second order system:

$$G_{ozw}(s) = \frac{D_{s_c}/2mC}{s^2 + 2z_3 w_3 s + w_3^2} \quad (88)$$

This result is not surprising since only the third mode is contributing to the system dynamics. The rigid body mode and the symmetric flexible mode do not affect the performance. In order to compute the closed loop transfer function, we recall equation (83) and apply it to the closed loop case, corresponding to the state space system SYS_czw (81):

$$G_{czw}(s) = \mathbf{C}_{czw} [s\mathbf{I} - \mathbf{A}_{czw}]^{-1} \mathbf{B}_{czw} + \mathbf{D}_{czw} \quad (89)$$

Since only mode 3 contributes to the performance, we can truncate modes 1 and 2 from \mathbf{A}_{czw} to obtain $\tilde{\mathbf{A}}_{czw}$. The matrix inversion can be written as:

$$[s\mathbf{I} - \tilde{\mathbf{A}}_{czw}]^{-1} = \begin{pmatrix} w_3^2 - \frac{3s_c}{m} \left(\frac{s}{K_p} + \frac{K_d}{t_d} \right) & -1 & 0 \\ -\sqrt{12/m} \cdot s_c & s + 2z_3 w_3 & \frac{3K_d}{\sqrt{12m} t_d^2} \\ & 0 & s + \frac{1}{t_d} \end{pmatrix}^{-1} \quad (90)$$

the other two matrices are then given as

$$\tilde{\mathbf{B}}_{c_{zw}} = \begin{bmatrix} 0 \\ 1/\sqrt{12m} \\ 0 \end{bmatrix}, \quad \tilde{\mathbf{C}}_{c_{zw}} = \begin{bmatrix} -6s_c & 0 & 0 \end{bmatrix}, \quad \tilde{\mathbf{D}}_{c_{zw}} = [0] \quad (91)$$

solving for the closed loop transfer function we get equation (92):

$$G_{c_{zw}}(s) = \frac{\frac{s_c t_d}{2} s + \frac{s_c}{2}}{m t_d s^3 + (2z_3 w_3 m t_d + m) s^2 + (2z_3 w_3 m + w_3^2 t_d m - 3s_c K_p t_d - 3s_c K_d) s + (m w_3^2 - 3K_p s_c)}$$

It can be seen that the transfer function is more complicated than in the open loop case and that the control gains K_d and K_p will affect the location of the closed loop transfer function poles. Figure 10 shows the closed loop (92) and open loop (88) transfer functions. The nominal values of all structural and control parameters are summarized in Appendix 1.

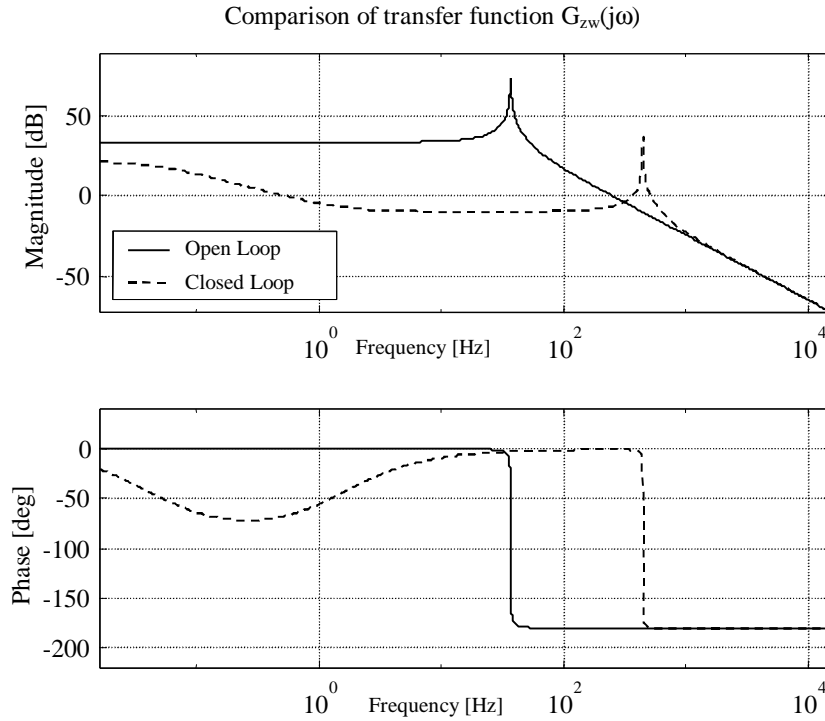


Fig.10: Comparison of open and closed loop $G_{zw}(j\omega)$

A look at stability is needed before concluding the integrated modeling section. Figure 11 shows that we have no poles in the right half-plane or on the $j\omega$ -axis in the open loop and closed loop cases. The system is asymptotically stable. A further analysis of root locus, Nyquist and Nichols plots are contained in the performance improvement memorandum (Part 4).

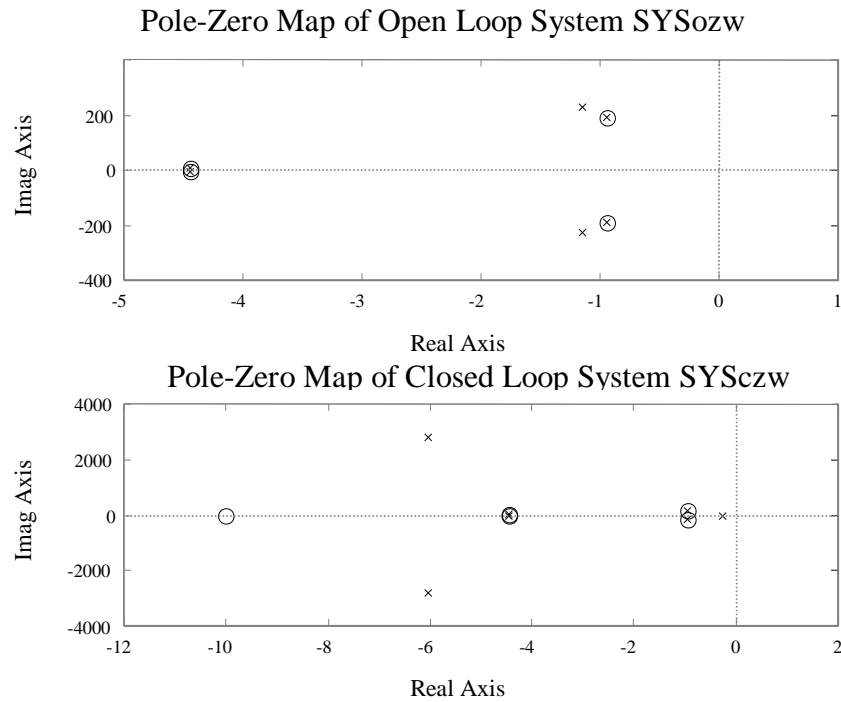


Fig.11: Pole-Zero Map for Open Loop and Closed Loop System

References

- [1] Gutierrez, H.; *Performance Assessment and Enhancement of Precision Controlled Structures During Conceptual Design*, Ph.D. thesis, Massachusetts Institute of Technology, February 1999
- [2] Crawley, E., Hall, S.; *The Dynamics of Controlled Structures*, 1991 Course notes manual, Massachusetts Institute of Technology, SERC Report # 10-91-I
- [3] DMK/DPK; *Formeln und Tafeln*, Unterrichtswerk der deutschschweizerischen Mathematikkommission und der deutschschweizerischen Physikkommission, 3. Auflage, Verlag Orell Fuessli, Zurich, Switzerland, 1984
- [4] Gross D., Messner D; *ADAM[®] Technology*, ABLE Engineering Information Binder, AEC-Able Engineering, Goleta, California, 1999
- [5] Craig, R.; *Structural Dynamics, An introduction to computer methods*, John Wiley & Sons, 1981
- [6] *Matlab 5.2 User Manual*, The Mathworks, 1998
- [7] Garnek, M., *EOS Orbital Damping Study*, GE Astro Space, MA93-EOS-002, March 31, 1993
- [8] Wirsching P., Paez T., Ortiz K., *Random Vibrations, Theory and Practice*, John Wiley & Sons, 1995
- [9] Feron, E., *Personal Class notes 16.31 Feedback Control Systems*, Massachusetts Institute of Technology, 1998
- [10] Dorf, Bishop; *Modern Control Systems*, 1997, page 662
- [11] *Optics Problem Solver*, REA Research Education Association, Problem Solver, 1997
- [12] Bélanger P.R.; *Control Engineering, A modern approach*, Saunders College Publishing, 1995
- [13] Redding, D; Breckenridge W.; *Optical Modeling for Dynamics and Control Analysis*, Paper Number AIAA-90-3383

Appendix 1

Nominal Parameter values

Appendix 2

MATLAB[™] diary session

Appendix 3

Matlab Script: sample_3dof_1.m

Appendix 1**Nominal Parameter values**

Mass parameter m	200 kg
Young's modulus E^4	$7.1 \cdot 10^{10}$ N/m ²
Cross sectional area A^5	0.001 m ²
Reference length l_o	10 m
Disturbance Rolloff ω_{RO}	100 Hz
Proportional Gain K_p	0.05
Derivative Gain K_d	0.01
Time Delay τ_d	0.1 sec
Output scale factor s_c	$1 \cdot 10^9$

Sample problem nominal model properties

Appendix 2

MATLAB™ session diary for script sample_3dof_1.m. The intent of this script is to be able to compare the numerically computed values for the system matrices with the analytically derived values.

```
sample_3dof_1
===== RESULTS 3DOF SAMPLE PROBLEM =====
Natural frequencies [Hz]: 0      29.9871      36.7265

PHI_orig =

    1    1    2
    1    0   -1
    1   -1    2
                                original PHI matrix (hand calc)

M_tilda_orig =

    1200         0         0
         0      400         0
         0         0      2400
```

⁴ Elastic modulus of aluminum [3]

⁵ Corresponds to 10 cm² cross sectional area, reasonable value for a large space truss [4]

PHI0 =

0.0289	-0.0500	0.0408
0.0289	-0.0000	-0.0204
0.0289	0.0500	0.0408

M_tilda_0 =

1	0	0
0	1	0
0	0	1

Cz =

1.0e+008 *						
0.0000	-0.0000	-1.2240	0	0	0	

Bu =

0
0
0
-0.0000
0.0500
0.0612

Cy =

1.0e+008 *						
-0.0000	0.0000	2.4480	0	0	0	

Ap =

1.0e+004 *						
0	0	0	0.0001	0	0	
0	0	0	0	0.0001	0	
0	0	0	0	0	0.0001	
-0.0039	0	0	-0.0009	0	0	
0	-3.5500	0	0	-0.0002	0	
0	0	-5.3250	0	0	-0.0002	

Bw =

0
0
0
0.0289
-0.0000
-0.0204

diary off

Appendix 3

```

% sample_3dof_1.m
% 3-DOF PRECISION SPACE OBSERVATORY SAMPLE PROBLEM
% A simple interferometer with a central mass (m2), two
% collectors (m1 and m3) and two interconnecting springs
% k1 and k2 is assumed.
%
% The goal of this sample problem is fourfold:
%
% 1. Clearly explain and demonstrate the steps and equations
% involved in creating an integrated dynamics model of a
% precision controlled structure, involving structures,
% optics and controls.
% 2. Explore three different methods for predicting performance
% RMS values: time-domain, frequency domain and Lyapunov
% 3. Verify the existing disturbance analysis, sensitivity
% and uncertainty analysis tools with a simple analytical
% example.
% 4. Analyze the level of insight that can be gained from a
% low-order model with 3-DOF that is at the limit of what
% can be expected to be solved analytically. Pave the way
% for further developments.
%
% Author:      Olivier de Weck
% Copyright:   Massachusetts Institute of Technology
% Date:       20 March 1999
% Memorandum: MIT-SSL-NGST-99-1

clear all
close all

% 1. Create Integrated Model
% =====

% 1.1 Structural Modeling and Normal Modes Analysis
% =====

m=200;      % mass parameter for structural model [kg]
m1=m;      % mass of left collector [kg]
m2=4*m;    % mass of combiner (center mass) [kg]
m3=m;      % mass of right collector [kg]
lo=10;     % length of left and right connecting truss [m]
E=71e9;    % Young's Modulus for truss [N/m^2]
A=0.001;   % equivalent cross sectional area of truss [m^2]
k=(E*A)/lo; % equivalent axial stiffness [N/m]
w=logspace(-1,5,5000); % create frequency vector for future calculations

K1=k*[1 -1; -1 1]; % stiffness matrix of left spring
K2=k*[1 -1; -1 1]; % stiffness matrix of right spring
K=zeros(3,3);      % initialize global stiffness matrix
K(1:2,1:2)=K(1:2,1:2)+K1 ; % assemble global stiffness spring 1
K(2:3,2:3)=K(2:3,2:3)+K2 ; % assemble global stiffness spring 2
M=[m1 0 0 ; 0 m2 0 ; 0 0 m3]; % assemble global mass matrix

```

```

[PHI,LAMBDA]=eig(K,M); % solve generalized eigenvalue problem
% Note: the length of the eigenvectors, which are the columns of
% PHI is automatically normalized to 1 in MATLAB.
wnat=sqrt(diag(LAMBDA));
freq=wnat/2/pi; % vector of natural frequencies [Hz]
freq(1)=round(freq(1)); % remove numerical error from RB mode
wnat(1)=round(wnat(1)); % remove numerical error from RB mode
disp('===== RESULTS 3DOF SAMPLE PROBLEM =====')
disp(['Natural frequencies [Hz]: ' num2str(freq)])
PHI_orig = round([PHI(:,1)*sqrt(3) PHI(:,2)*(-1)*sqrt(2) PHI(:,3)*3])
% The above command recovers the original eigenvector matrix obtained
% from the hand calculations
M_tilda_orig = round(PHI_orig'*M*PHI_orig)
M_tilda=round(PHI'*M*PHI); % Creates the diagonal modal mass matrix
PHI0=PHI*inv(sqrt(M_tilda)) % Creates the mass normalized PHI matrix
M_tilda_0=round(PHI0'*M*PHI0) % Mass normalized modal masses are all 1
OMEGA=sqrt(LAMBDA); % equal to sqrt(PHI0'*K*PHI0) in [rad/sec]
zetal=0.005; zeta2=0.005; zeta3=0.005; % Assumed modal damping ratios
Z=diag([zetal zeta2 zeta3]); % Modal damping matrix
Ap=[zeros(3,3) eye(3); -OMEGA.^2 -2*Z*OMEGA]; % State transition matrix

```

% 1.2 Optics Modeling

```

% =====
% This step is very simplified in this sample problem. The optical
% performance metric is the OPD between the left and right optical
% light paths. The Czx matrix is the linear sensitivity matrix relating
% the physical DOF's of the structure to some optical performance
% metric. Here this is very simple as OPD=(l0+x2-x1)-(l0+x3-x2), thus
sc=1e9; % scale optics matrix to nm
Czx=sc*[ -1 2 -1 ];
Cz= [Czx*PHI0 zeros(1,3)]
Dzw= [0]; Dzu=[0];
% Assuming a wavelength of 7 microns and a requirement of lambda/6000
% on the OPD (1 sigma) to achieve satisfactory fringe visibility, we
% can obtain the performance requirement in [nm] as
opd_req=7e-6*sc/60;

```

% 1.3 Controls Modeling

```

% =====
% This encompasses choosing appropriate Sensors (Cyx), Actuators (Betau)
% and a stable compensator [Ac,Bc,Cc,Dc], which relates the sensor output
% y to the control input u
Betau=[0 -1 1]'; % Input Influence Coefficient Matrix (active strut)
Bu=[zeros(3,1); PHI0'*Betau] % Input Matrix in modal coordinates
Dyu=[0]; Dyw=[0]; % No feedthrough terms
Cyx = sc*[ 2 -4 2 ]; % Output Influence matrix (Sensor is laser metrology)
Cy = [Cyx*PHI0 zeros(1,3)] % Output matrix - sensor output is 2*OPD in nm
% Assume PD-controller (SISO) with time delay for active strut
Kp=-0.01; % Proportional Gain (negative displacement feedback)
Kd=-0.05; % Derivative Gain (negative rate feedback)
taud=0.1; % time delay [sec]
numc=[Kp*taud+Kd Kp]; denc=[taud 1] ; % Controller t.f. (neg feedback)
[magH, phaseH]=bode(numc,denc,w); % Controller TF evaluated
al=Kp*taud+Kd; ao=Kp; bl=taud; bo=1; % Controller TF coefficients
Ac=[-bo/bl]; Bc=[1]; % PD controller in state space

```

```

Cc=[(ao*b1-a1*bo)/b1^2]; Dc=[a1/b1]; % see Matlab tf2ss.m function
%
% Furthermore it is clear that the Ap-matrix is near singular, which
% can be seen by the high conditioning number of Ap. Without modeling
% the ACS in detail we assume here that an ACS is on line during ob-
% servations and that it has a finite bandwidth wacs and critical
% damping zacs, which stabilizes the rigid body mode.
Ap_cond= cond(Ap); % Condition number of plant A matrix
wacs=1*2*pi; % Assume 1 Hz bandwidth of ACS controller
zacs=.707 ; % critical damping for ACS
Ap(4,1)=-wacs^2; Ap(4,4)=-2*zacs*wacs % ACS acts on Ap matrix

% 1.4 Disturbance Source Modeling
% =====
% Disturbance Source is first modeled as a shaping filter transfer
% function Gwd, which can be used to compute the PSD's or can be
% transformed into state space form for Lyapunov analysis
Betaw=[0 1 0]'; % Disturbance Influence Matrix (w enters at combiner)
Bw=[zeros(3,1); PHI0'*Betaw] % Disturbance matrix in modal coordinates
Dyw=[0]; Dzw=[0]; % The disturbance feedthrough terms are zero
wro=100*2*pi; % disturbance force rolloff frequency is 100 Hz
numGwd1=[wro]; denGwd1=[1 wro]; % lowpass transfer function
[magGwd1,phaseGwd1]=bode(numGwd1,denGwd1,w); % Evaluate Gwd1 (LPF)
Sww1=magGwd1.^2; % Compute Disturbance PSD's
Ad1 = [-wro]; Bd1=[1]; % Disturbance 1 in state space
Cd1 = [wro]; Dd1=[0]; % form (LPF) - 1 state
% Bandpass Filter Noise Model for future expansion of this code
wru=1*2*pi; % disturbance force rollup frequency is 1 Hz
numGwd2=[wro 0]; denGwd2=[1 wro+wru wro*wru]; % bandpass transfer function
[magGwd2,phaseGwd2]=bode(numGwd2,denGwd2,w); % Evaluate Gwd2 (BPF)
Sww2=magGwd2.^2;
Ad2 = [0 1 ; -wru*wro -wru-wro]; % Disturbance 2 in state space
Bd2 = [ 0 1 ]'; % controller canonical form
Cd2 = [ 0 wro] ; Dd2=[0]; % (BPF) - 2 states

% 1.5 Integrated Model
% =====
% Integrated modeling means to assemble the results from the above
% modeling tasks into a form, which represents the closed-loop or
% open-loop behaviour of the system. This can be represented by the
% Gzw transfer function matrix or alternatively by the (Azd,Bzd,Czd,Dzd)
% state space system.
% SYS_ozw : Open loop system from shaped disturbance w to performance z
% SYS_czw : Closed loop system from shaped disturbance w to performance z
% SYS_ozd : Open loop system from white noise d to performance z
% SYS_czd : Closed loop system from white noise d to performance z

Aozw=Ap; Bozw=Bw; Cozw=Cz; Dozw=Dzw;
SYS_ozw = ss(Aozw,Bozw,Cozw,Dozw);
[magGozw,phaseGozw]=bode(SYS_ozw,w);

Aczw=[Ap+Bu*Dc*Cy Bu*Cc; Bc*Cy Ac];
Bczw=[Bw ; 0]; Cczw=[Cz 0]; Dczw=[0];
SYS_czw = ss(Aczw,Bczw,Cczw,Dczw);

```

```

[magGczw,phaseGczw]=bode(SYS_czw,w);

Aozd=[Ad1 zeros(1,6); Bw*Cd1 Ap];
Bozd=[Bd1; zeros(6,1)]; Cozd=[0 Cz]; Dozd=[0];
SYS_ozd = ss(Aozd,Bozd,Cozd,Dozd);
[magGozd,phaseGozd]=bode(SYS_ozd,w);

Aczd=[Ad1 zeros(1,6) 0; Bw*Cd1 Ap+Bu*Dc*Cy Bu*Cc; 0 Bc*Cy Ac];
Bczd=[Bd1 ; zeros(6,1); 0]; Cczd= [0 Cz 0]; Dczd=[0];
SYS_czd= ss(Aczd,Bczd,Cczd,Dczd);
[magGczd,phaseGczd]=bode(SYS_czd,w);

% Plot open loop and closed loop transfer functions

h_tf=figure;
set(h_tf, 'Name', 'Transfer Function Comparison 3DOF', 'Position', ...
    [100 200 500 400])
subplot(211)
semilogx(w/2/pi, 20*log10(abs(squeeze(magGozw))), 'k-', ...
    w/2/pi, 20*log10(abs(squeeze(magGczw))), 'k-.');
grid on, axis([min(w/2/pi) max(w/2/pi) ...
    min(20*log10(abs(squeeze(magGozw)))) ...
    1.2*max(20*log10(abs(squeeze(magGozw)))) ])
xlabel('Frequency [Hz]'), ylabel('Magnitude [dB]')
legend('Open Loop', 'Closed Loop', 3)
title('Comparison of transfer function G_z_w(jw)')
subplot(212)
semilogx(w/2/pi, squeeze(phaseGozw), 'k-', ...
    w/2/pi, squeeze(phaseGczw), 'k-.')
xlabel('Frequency [Hz]'), ylabel('Phase [deg]')
grid on
axis([min(w/2/pi) max(w/2/pi) -220 40])

% Analyze System Stability and Margins

figure
subplot(211), pzmap(SYS_ozw), temp=axis; axis([-15 0 temp(3:4)])
title(' Pole-Zero Map of Open Loop System SYS_ozw ')
subplot(212), pzmap(SYS_czw), temp=axis; axis([-15 0 temp(3:4)])
title(' Pole-Zero Map of Closed Loop System SYS_czw ')

%%%%%%%%%% END OF PART 1 %%%%%%%%%%%

```